

A Redox Role for the [4Fe4S] Cluster of Yeast DNA Polymerase δ

Phillip L. Bartels¹, Joseph L. Stodola²,
Peter M.J. Burgers^{2,*}, and Jacqueline K. Barton^{1,*}

Supporting Information

DNA synthesis and purification for electrochemistry. Thiol-modified DNA sequences were prepared by standard phosphoramidite chemistry on a DNA synthesizer (Applied Biosystems) using A, G, C, T phosphoramidites and the 3'-Thiol-Modifier 6-S-S CPG as purchased from Glen research. DNA substrates were cleaved and deprotected by 8-hour incubation in NH_4OH (Sigma-Aldrich) at 65 °C. Deprotected DNA was separated from truncation products by reverse-phase HPLC (Agilent PLRPS column, gradient of 5 – 75% ACN/95 - 25% 50 mM NH_4Ac over 30 minutes at a 2 mL/min flow rate). Thiol-modified DNA was reduced by dissolving in 50 μL Tris, pH 8.0 (Qiagen elution buffer), adding excess DTT (Sigma-Aldrich), and shaking for 45 minutes. DTT was removed by filtration through a NAP-5 column (GE Healthcare) prior to a final round of HPLC purification (gradient of 5 – 15% ACN/95 – 85% 50 mM NH_4Ac over 35 minutes at 2 mL/min). Lastly, single-stranded DNA was desalted by standard ethanol precipitation (100 μl water, 1 mL 100% EtOH, 130 mM NaCl) and the identity of the substrate was confirmed by MALDI-TOF. Unmodified oligomers were ordered from IDT and purified by the DMT-free HPLC method. Desalted DNA was dissolved in a phosphate storage

buffer (5 mM sodium phosphate, 50 mM NaCl, pH 7.0) and concentrations were determined by UV-visible spectroscopy using ϵ_{260} values estimated by Integrated DNA Technologies (IDT). Equimolar concentrations of single stranded DNA were then degassed and annealed (rapid heating to 95° C, 5-minute incubation, and 1.5 hour cooling to 20° C).

Preparation of DNA-modified Gold Electrodes. Multiplexed chips containing 16 Au electrodes (0.015 cm² area) were prepared as described previously (64). Self-assembled monolayers (SAMs) were formed by incubating 25 μ L of 25 μ M duplexed DNA on the electrode overnight, after which electrodes were rinsed 3-5 times in phosphate buffer (5 mM sodium phosphate, pH 7.5, 50 mM NaCl) and backfilled for 45 minutes with 1 mM 6-mercapto-1-hexanol (Sigma-Aldrich) in the same buffer containing 5% (v/v) glycerol. Electrodes were then extensively rinsed in phosphate buffer followed by protein storage buffer (30 mM HEPES, pH 7.4, 350 mM NaAc, 1 mM DTT, 0.1 mM EDTA, 10% glycerol, and 0.01% decaethylene glycol monododecyl ether). Lastly, the absence of electroactive impurities was confirmed by scanning the surface with cyclic voltammetry (CV).

Bulk electrolysis experiments were undertaken by droplet electrochemistry (30-40 μ L solution) on Au rod electrodes of 0.0314 cm² electrode area (Pine Research Instrumentation). Electrodes were cleaned as previously described (65), and monolayers formed using the same procedure as the multiplexed chip.

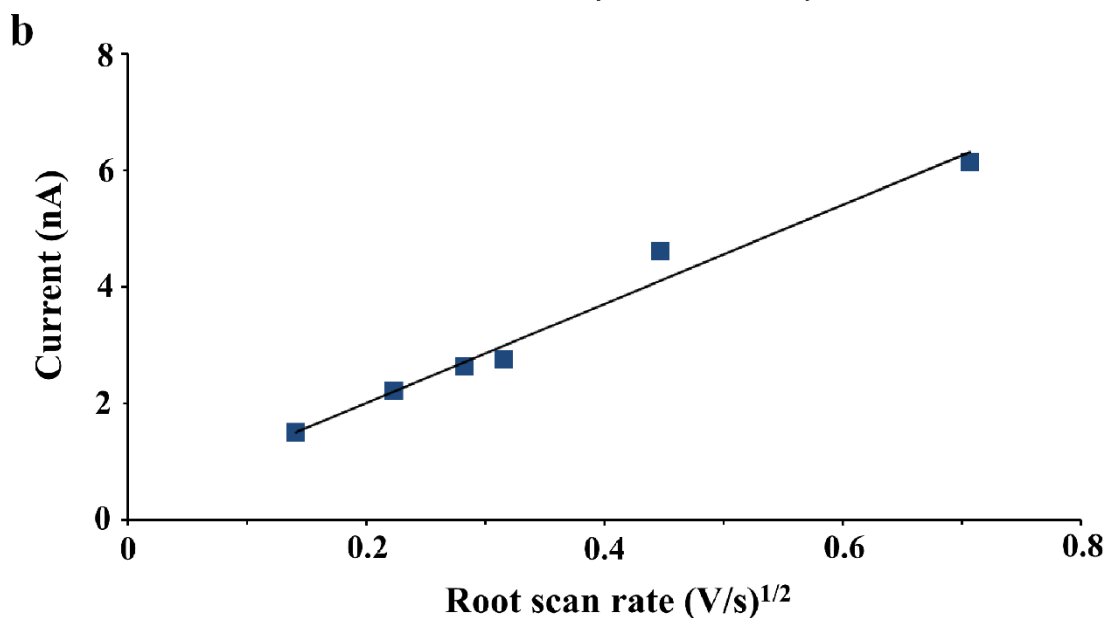
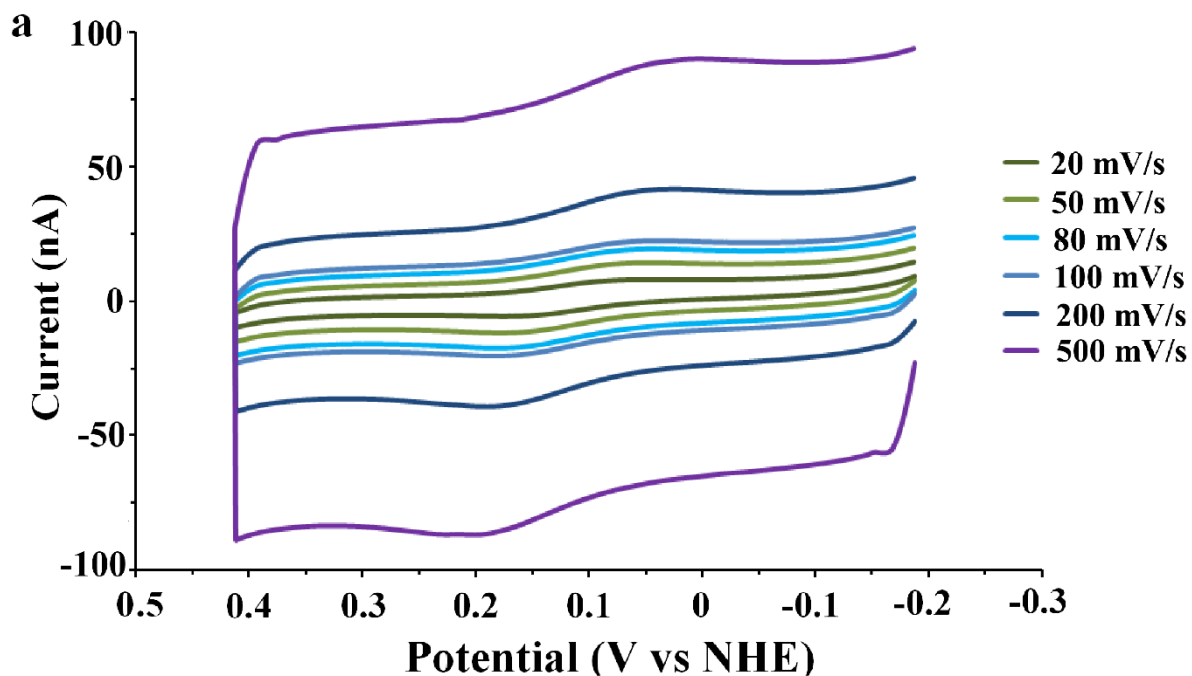


Figure S1. Scan rate dependence of the CV current in 500 nM Pol δ DV incubated with 5.0 μ M PCNA, 80 μ M dATP, and 8.0 mM MgAc₂. (a) The maximum peak current increases with increasing scan rate, coupled with an increase in peak splitting. (b) The current exhibits a linear dependence on the square root of the scan rate, characteristic of a diffusive rather than adsorbed species. The scan rates included are 20, 50, 80, 100, 200, and 500 mV/s. The line was fit to data averaged from 8 separate experiments, and the fit is $I = 7.7559v^{1/2} + 0.5725$ with an R^2 value of 0.9828.

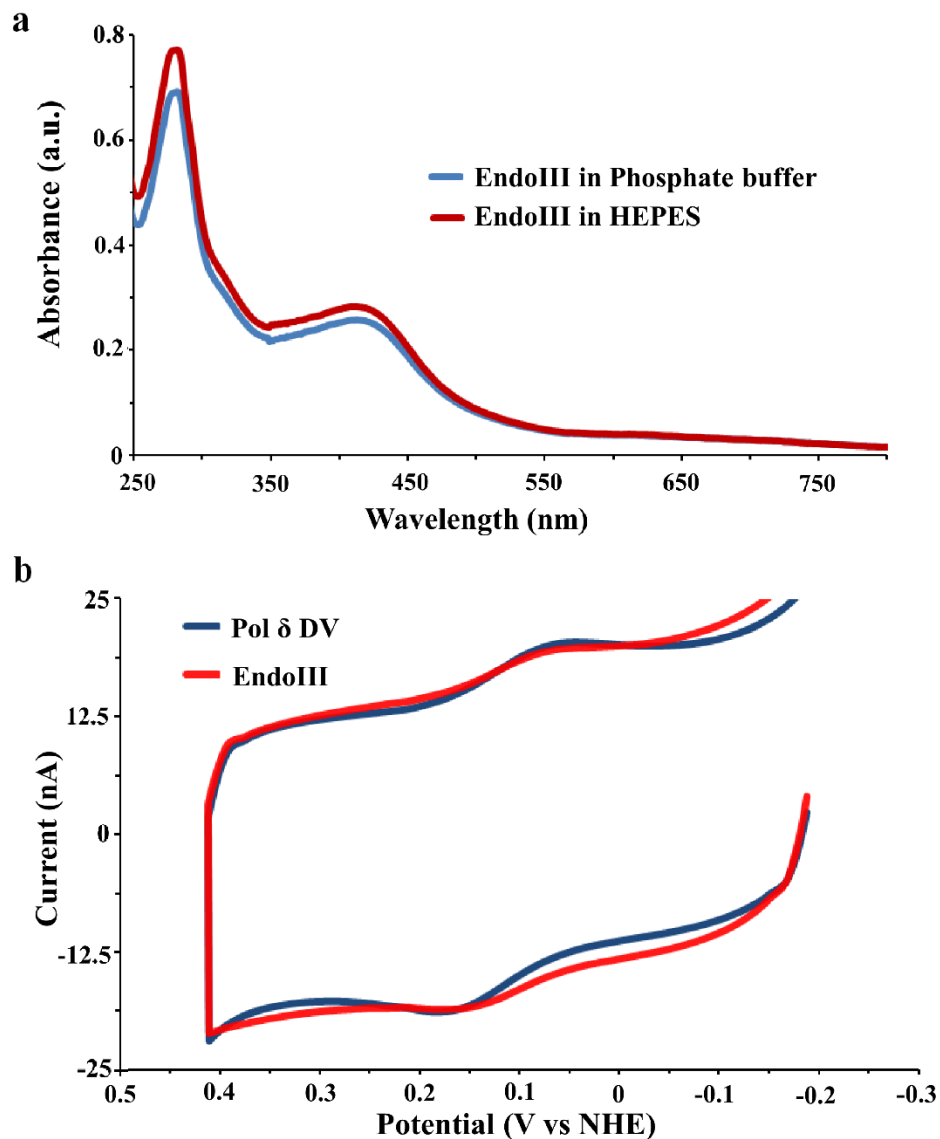


Figure S2. Pol δ and EndoIII electrochemistry compared. 1.5 μM EndoIII (stored in 20 mM sodium phosphate, pH 7.5, 150 mM NaCl, 1 mM EDTA) was exchanged into Pol δ storage buffer (30 mM HEPES, pH 7.4, 350 mM NaAc, 1 mM DTT, 0.1 mM EDTA, 10% v/v glycerol, 0.01% decaethylene glycol monododecyl ether w/v) and added to a multiplexed chip containing unmodified Pol δ DNA (49:58-mer substrate). (a) UV-visible spectra taken before and after buffer exchange confirm the stability of EndoIII in a HEPES-based buffer. (b) The midpoint potential as measured by CV is 113 ± 3 mV, virtually indistinguishable from Pol δ DV at 113 ± 5 mV versus NHE.

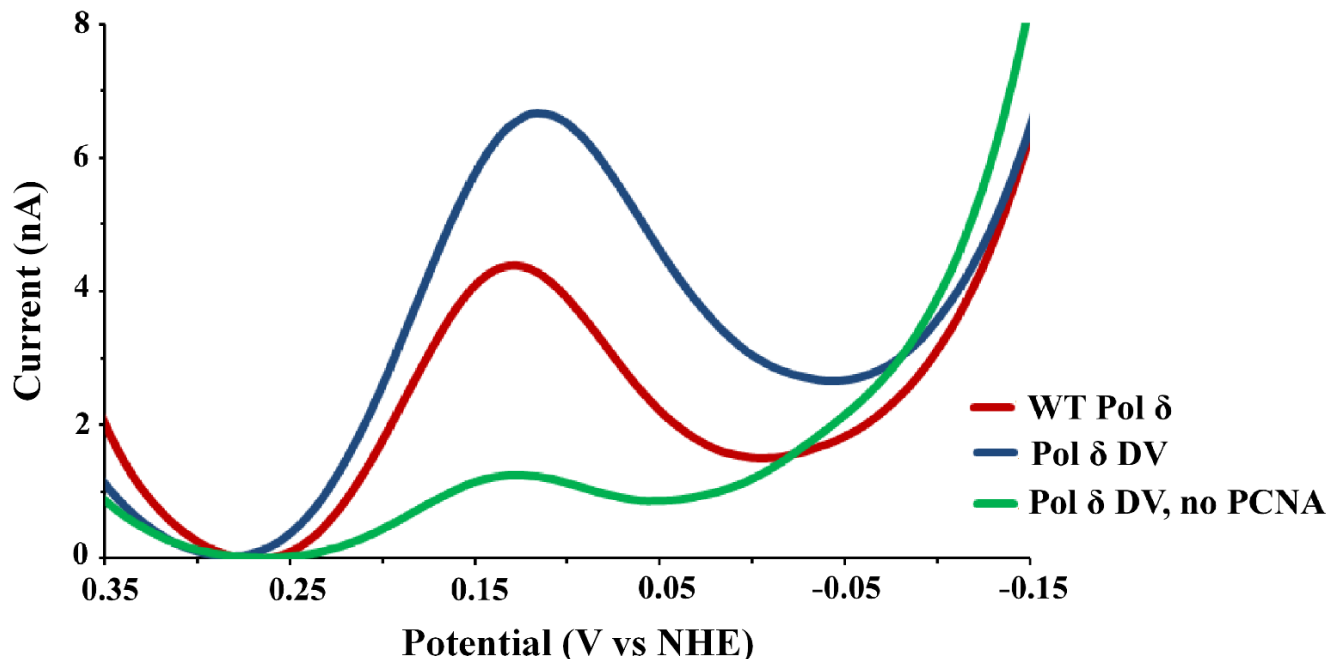


Figure S3. SQWV of 500 nM WT Pol δ and exonuclease-deficient Pol δ DV with and without 5.0 μ M PCNA. WT and exo^- Pol δ DV share the same potential, and both generate a substantial signal on a DNA-modified gold electrode; the smaller size of the WT signal may be due in part to DNA degradation by exonuclease activity. PCNA itself does not affect the potential, but its absence results in significantly decreased signal size and lower stability over time. SQWVs were taken at 15 Hz frequency and 25 mV amplitude, and electrochemistry was carried out in storage buffer (20 mM HEPES, pH 7.4, 350 mM NaAc, 1 mM DTT, 0.1 mM EDTA, 10% glycerol v/v, 0.01% decaethylene glycol monododecyl ether v/v) with 8.0 mM MgAc_2 and 80 μ M dATP.

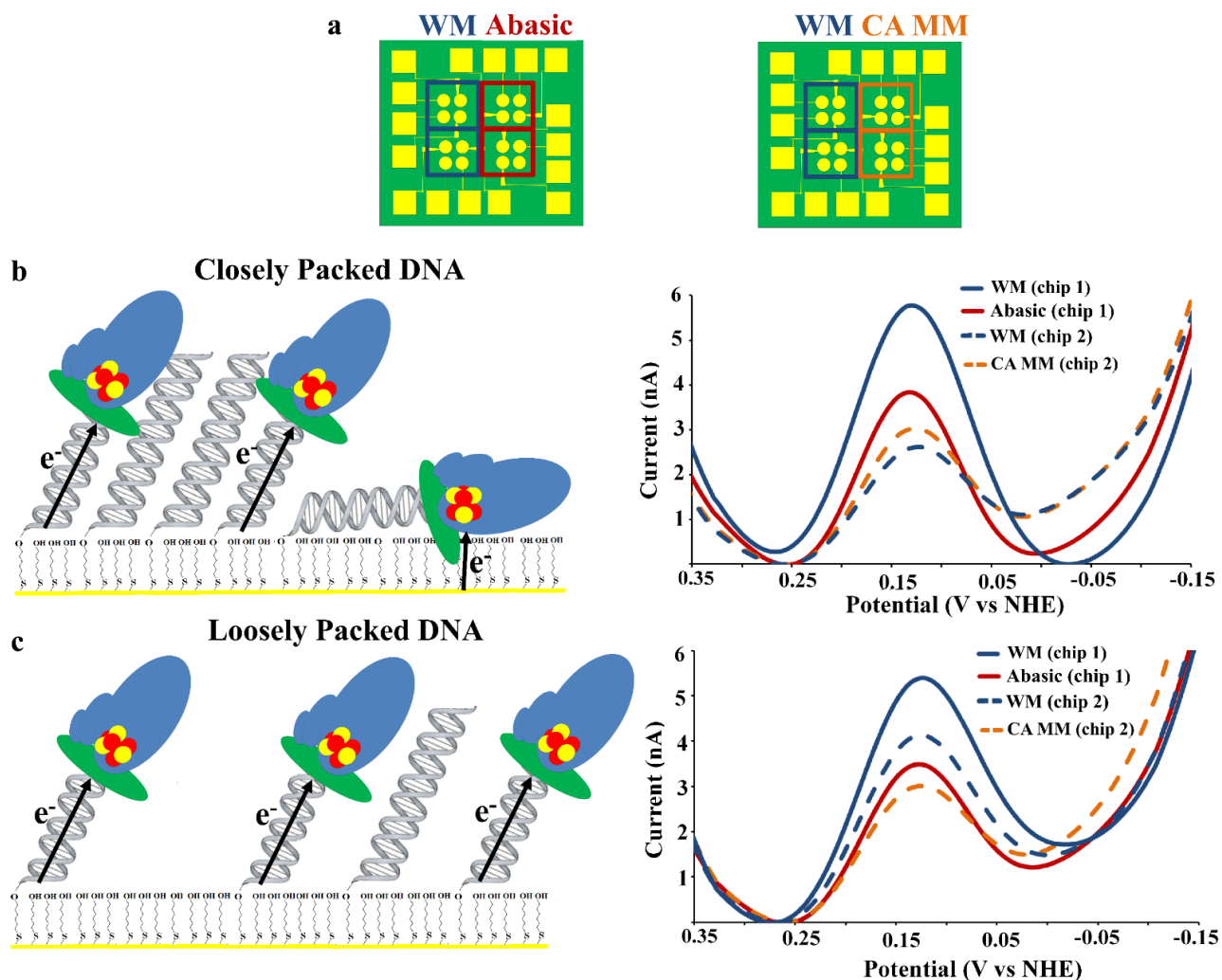


Figure S4. Pol δ electrochemistry on different DNA monolayer morphologies. (a) To find an optimal DNA monolayer morphology for Pol δ signaling, we prepared multiplexed chips containing either closely packed (assembled with 100 mM MgCl₂) or loosely packed (no MgCl₂) DNA films. Two chips were prepared for both morphologies, with one half of each chip consisting of well-matched (WM) DNA (dark blue) and the other containing DNA with either an abasic site (red) or a CA mismatch (orange) 6 nucleotides from the monolayer surface. (b) On closely packed films, Pol δ SQWV signals were highly variable and showed $46 \pm 33\%$ attenuation on abasic DNA (solid SQWV traces) but no significant mismatch discrimination (dashed SQWV traces). (c) In contrast, SQWV signals on loosely packed films were much more consistent between electrodes, with a $44 \pm 16\%$ signal loss on abasic DNA (solid traces) and $46 \pm 29\%$ signal loss with CA mismatch DNA (dashed traces). To minimize the effects of variability between devices, all direct comparisons were made on a single chip; scans that were directly compared are denoted by either solid or dashed lines in the SQWV signals shown. The SQWV traces shown are an average of 6 individual electrodes on a single device, with scans taken at 15 Hz frequency and 25 mV amplitude.

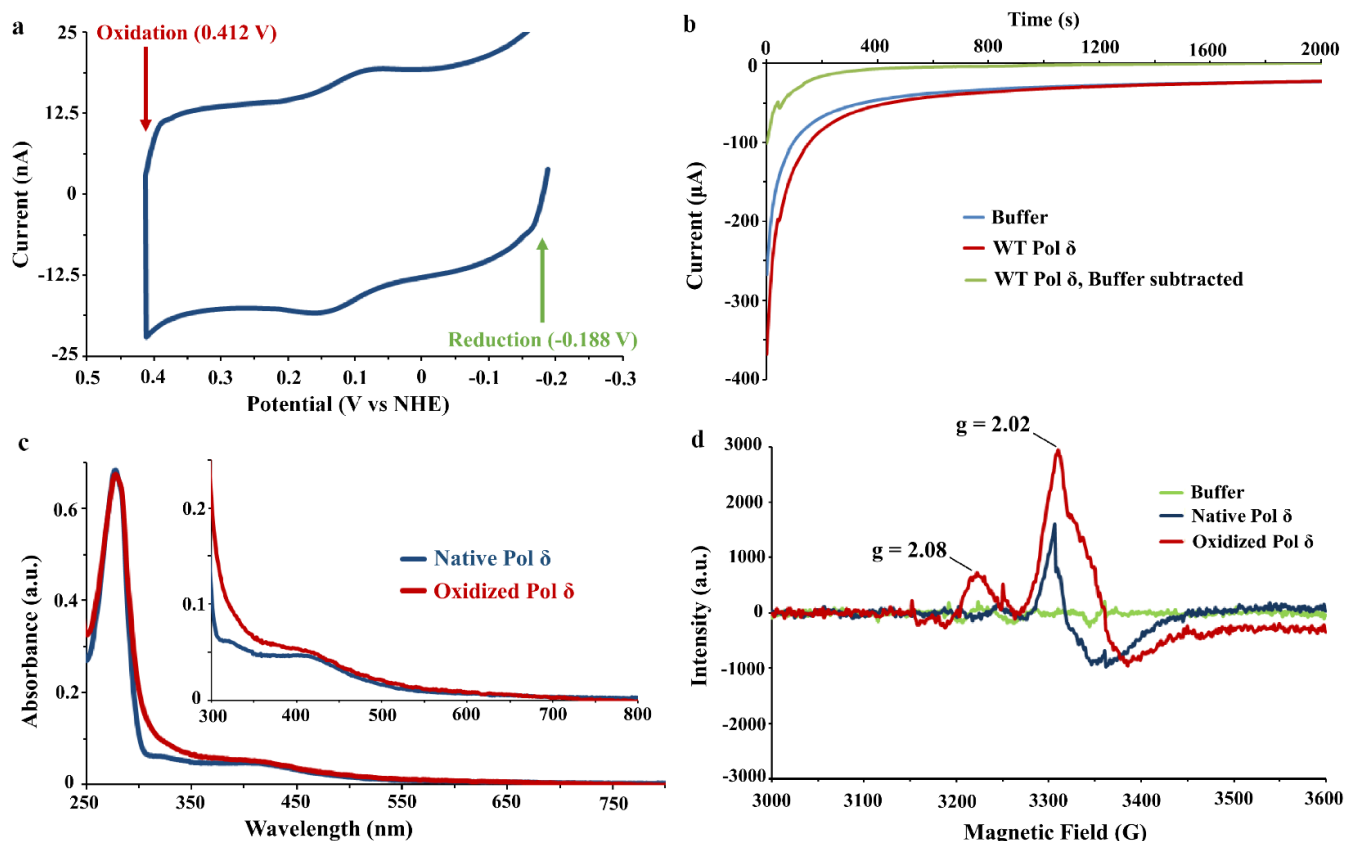


Figure S5. Characterization of electrochemically oxidized Pol δ . **(a)** Bulk electrolysis potentials were ~ 200 mV beyond the major oxidative and reductive peaks at 0.412 V (oxidation) and -0.188 V (reduction) versus NHE. **(b)** Yields were calculated by subtracting a background electrolysis (blue) from one containing protein (red) and taking the area under the resultant curve (green). Electrolysis of 150 μL of 2.74 μM Pol δ at 0.412 V gave $\sim 35\%$ oxidation yield. **(c)** UV-visible spectra reveal an increased absorbance from 300-400 nm consistent with cluster oxidation with no evidence of protein aggregation. **(d)** CW X-band EPR spectra at 10 K reveal the presence of both $[\text{4Fe4S}]^{3+}$ ($g = 2.08$) and $[\text{3Fe4S}]^+$ ($g = 2.02$) species in the oxidized sample, with a residual amount of $[\text{3Fe4S}]^+$ cluster present in the native sample. These results are consistent with the formation of $[\text{4Fe4S}]^{3+}$ cluster after anaerobic bulk electrolysis, with some degrading to form $[\text{3Fe4S}]^+$ cluster in the absence of DNA. As slight sample loss did occur following oxidation, the UV-visible spectrum of oxidized Pol δ has been normalized to native absorbance at 280 nm to afford a more direct comparison. EPR spectra were taken at 12.85 mW microwave power, 2 G modulation amplitude, and a receiver gain of 5.02×10^3 .

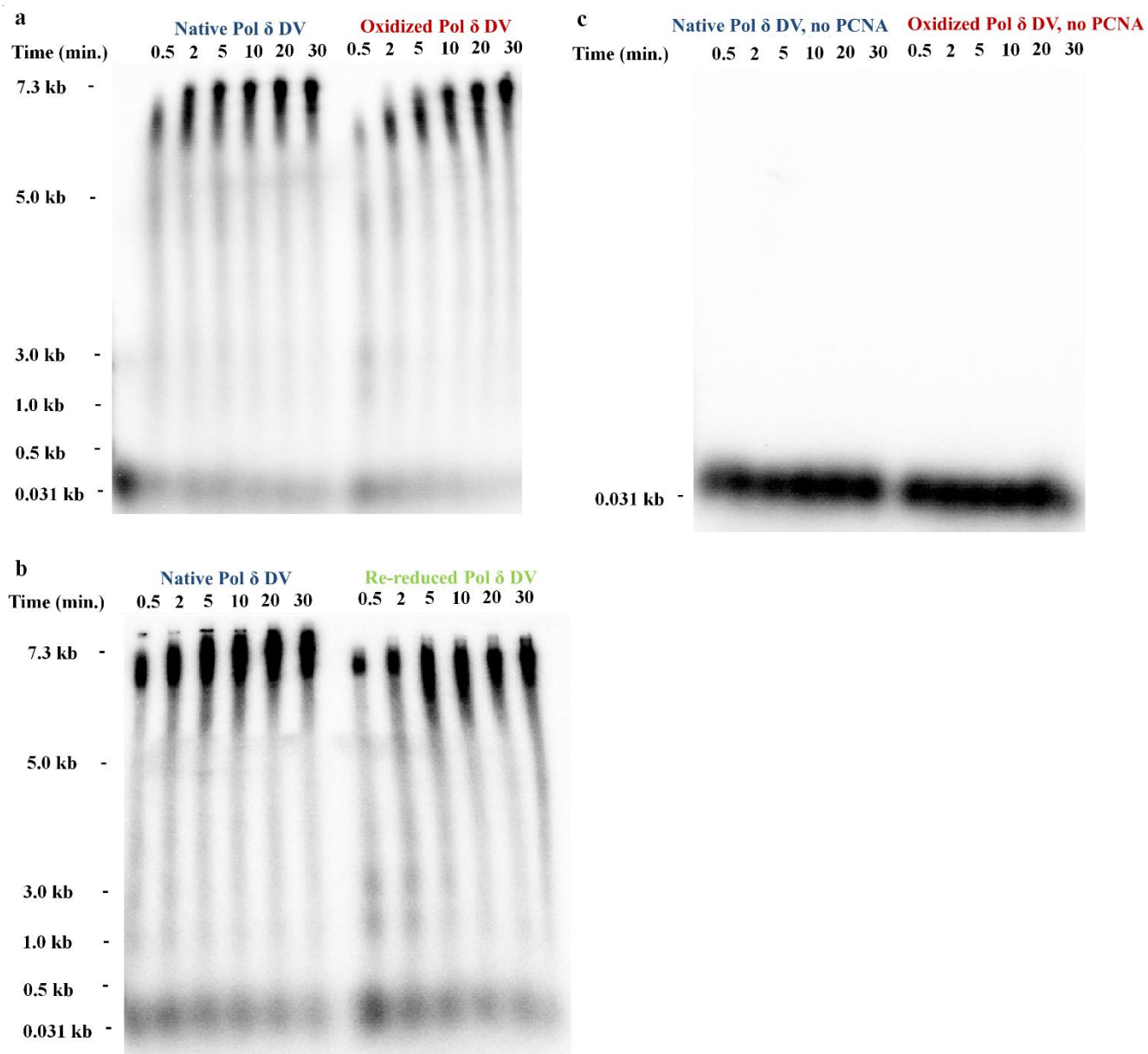


Figure S6. Complete alkaline agarose gels from Figure 2 and control lacking PCNA. The gels include untreated and oxidized Pol δ DV with 5.0 nM PCNA (**a**), untreated and re-reduced Pol δ DV (**b**), and untreated and oxidized Pol δ DV in the absence of PCNA (**c**). No DNA synthesis occurs in the absence of PCNA, confirming that the observed activity in native and oxidized samples is processive.

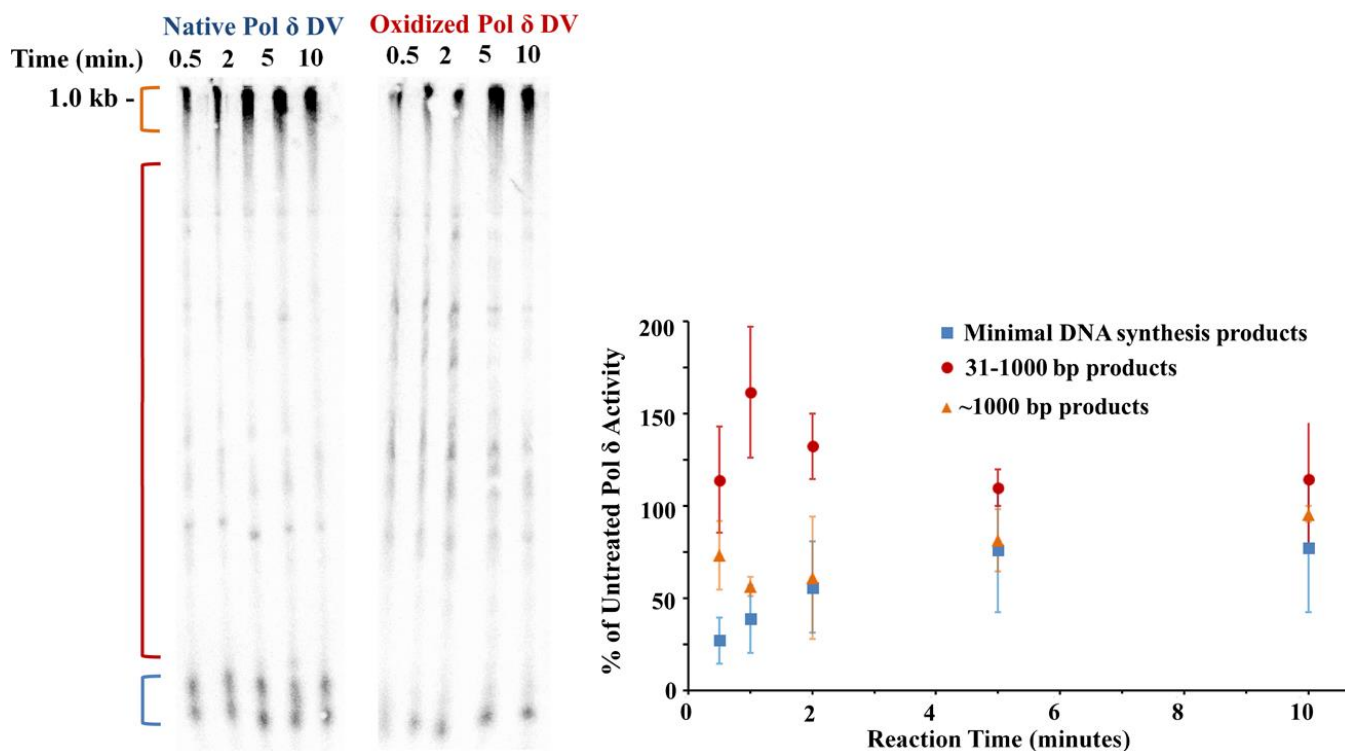


Figure S7. Establishment of activity by oxidized Pol δ . To see if oxidized Pol δ remained active or stalled completely, 0.01% heparin was included in reactions to challenge synthesis and products were analyzed on a 5% denaturing polyacrylamide gel to resolve DNA between 30 and 1000 bp (left). Pol δ remains active after oxidation, primarily forming intermediate-sized products (red range on gel). Native Pol δ is more sensitive to heparin, with more DNA close to primer length (blue range), but when it does associate with DNA, most products are around the maximum size (orange range). These results are consistent with tighter binding and slower processive DNA synthesis by the oxidized form. Gels were quantified using ImageQuant software; as synthesis appears as smears at this resolution, the total amount of background-subtracted radioactivity in each major range shown was compared between untreated and oxidized Pol δ . Error bars are standard deviation of the mean ($n = 3$).

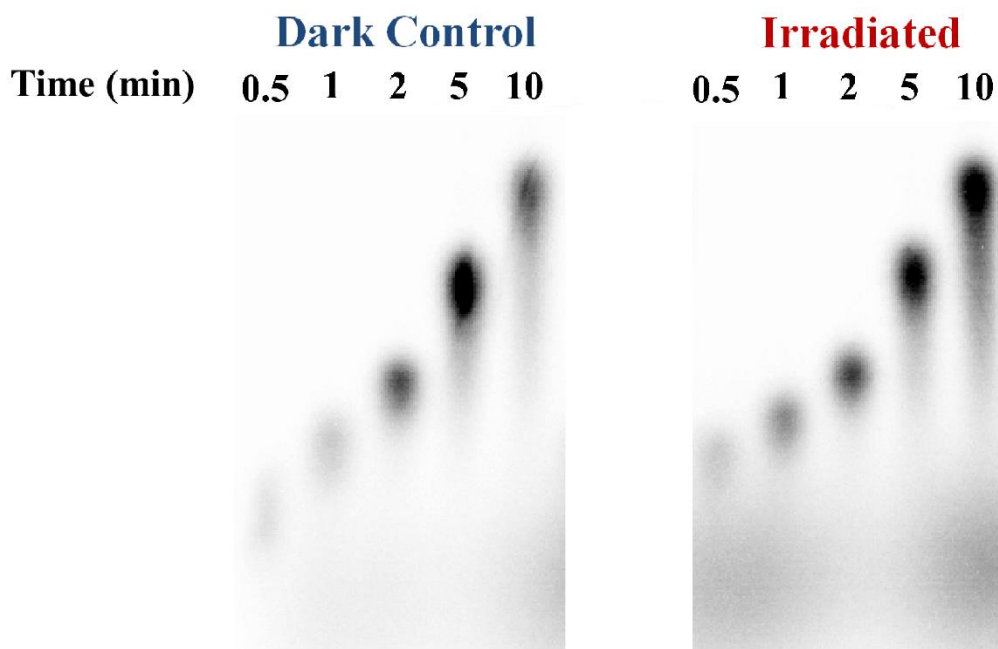


Figure S8. AQ assay controls with 140 nM *E. coli* Klenow fragment exo^- . UVA irradiation in the presence of AQ-primed DNA had no significant effect on DNA synthesis by Klenow fragment. The lack of difference confirms that irradiation in the presence of AQ does not adversely affect polymerase enzymes, and further supports the assignment of attenuated activity in Pol δ under the same conditions to [4Fe4S] cluster oxidation.

SI References

- (64) Slinker, J. D.; Muren, N. B.; Gorodetsky, A.A.; Barton, J. K. *J. Amer. Chem. Soc.* **2010**, *132*, 2769–2774.
- (65) Barton, J.K.; Bartels, P.L.; Deng, Y.; O’Brien, E. *Methods Enzymol.* **2017**, *591*, 355–414.